NIH RELAIS Document Delivery

NIH-10286720

JEFFDUYN

NIH -- W1 MA34IF

JOZEF DUYN
10 Center Dirve
Bldg. 10/Rm.1L07
Bethesda, MD 20892-1150

ATTN:
PHONE: 301-594-7305
FAX: -
E-MAIL:

SUBMITTED: 2002-08-29 17:22:18
PRINTED: 2002-09-05 07:56:01
REQUEST NO.:NIH-10286720
SENT VIA: LOAN DOC
7967429

NIH Fiche to Paper Journal

TITLE: MAGNETIC RESONANCE IN MEDICINE : OFFICIAL JOURNAL OF THE SOCIETY OF MAGNETIC RESONANCE IN MEDICINE / SOCIETY OF MAGNETIC RESONANCE IN MEDICINE
PUBLISHER/PLACE: Wiley-Liss, Inc., a division of John Wil New York, NY :
VOLUME/ISSUE/PAGES:1993 Oct;30(4):409-14 409-14
DATE: 1993
AUTHOR OF ARTICLE: Duyn JH; Moonen CT
TITLE OF ARTICLE: Fast proton spectroscopic imaging of human brain u
ISSN: 0740-3194
OTHER NOS/LETTERS: Library reports holding volume or year
8505245
8255188
SOURCE: PubMed
CALL NUMBER: W1 MA34IF
REQUESTER INFO: JEFFDUYN
DELIVERY: E-mail: jhd@helix.nih.gov
REPLY: Mail:

Fast Proton Spectroscopic Imaging of Human Brain Using Multiple Spin-Echoes

Jeff H. Duyn, Chrit T. W. Moonen

We introduce a multi-echo multi-slice MR proton spectroscopic imaging method, which allows for a dramatic reduction of the measurement time by acquiring multiple spin-echoes within a single repetition time. In the multi-echo multi-slice experiment discussed in this paper, a threefold reduction in measurement time is obtained by sacrificing some spectral resolution. Signal-to-noise ratio and spatial resolution are preserved. Metabolite images of *N*-acetyl aspartate, and total choline + total creatine from multiple slices through the human brain are presented and compared with images obtained with a conventional single-echo multi-slice method.

Key words: proton spectroscopic imaging; brain, MR; fast MR imaging.

INTRODUCTION

In recent years, significant advances have been made in proton spectroscopic imaging (HSI) techniques and their application to the mapping of metabolite levels in human brain (1–16). HSI studies proved successful in showing locally changed levels of metabolites in various pathologies including chronic and acute brain infarction (8, 9), multiple sclerosis (10, 11), epilepsy (12), brain tumors (13–15), and acquired immunodeficiency syndrome (16).

Most HSI techniques use gradient phase encoding to obtain spectra from one-, two- (1–3, 6–12), or even three-dimensional (4, 5) arrays of voxels simultaneously. This is at the cost of only a slight reduction in the signal-to-noise ratio (SNR) (17) per unit volume and unit time, as compared with single voxel methods. Although three-dimensional (3D) HSI allows mapping of a large brain volume, the vast number of phase encoding steps makes its duration prohibitive for most clinical applications. Recently, as an alternative, multi-slice 2D HSI techniques were introduced (6, 7), reducing the total measurement time as compared with the 3D experiment while preserving the ability to obtain metabolic information simultaneously from multiple slices.

Most clinical HSI studies sample a spin-echo signal at long echo times (*TE* 136–272 ms), at which the unwanted resonances of lipid and water are attenuated significantly due to T_2 decay. For the metabolites of interest (NAA, choline, creatine, and lactate), signal decay due to intravoxel susceptibility effects is generally significantly larger than that due to T_2 relaxation effects ($T_2^* << T_2$) In these cases, the data collection efficiency can be increased by acquiring multiple spin-echoes (18–21). The increased efficiency could then be applied to increasing SNR or to reduce the measurement time. Here, we show that the latter application can be realized on a conventional whole-body scanner.

METHODS

Measurements were performed on a normal volunteer using a conventional 1.5T GE/SIGNA whole-body scanner (GE Medical Systems, Milwaukee) with 10 mT/m actively shielded gradients and a standard quadrature head coil. The pulse sequence of the multi-spin-echo experiment was based on the single spin-echo multi-slice experiment described by Duyn *et al.* (6). The multi-spin-echo sequence consisted (Figs. 1a and 1b) of three parts: a chemical shift selective saturation (CHESS) sequence for water suppression, multiple-slice outer volume suppression (OVS), and a multi spin-echo SI sequence. The CHESS sequence (Fig. 1a) was identical to that used in the single-echo method. The OVS sequence (Fig. 1b) was a shortened version of the sequence described previously (6), and a delay of 6 ms was added to minimize the effects of eddy currents (see Discussion). The multi spin-echo sequence (Fig. 1a) acquired four spin-echoes at equidistant intervals of 148 ms. The first echo was positioned at 200 ms to reduce lipid contamination. This was done by using an additional 180° RF pulse. Thus, one slice selective 90° and five slice selective 180° RF pulses were used. The bandwidth of the pulses was 2 kHz. The 180° pulses selected a 10% thicker slice than the 90° RF, resulting in an improved slice profile. The resulting slice profile had a full width at half maximum of 13 mm (Fig. 1c). A 7 mm slice gap was maintained between adjacent slices. The 180° RF pulses were flanked by 4-ms gradient crusher pulses in x, y, and z direction, the x and y components being mT/m. The strength of the z-crusher was varied between −9, −3, 3, 9, and −6 mT/m on subsequent crusher pairs in order to suppress stimulated echoes (22) and higher order spin-echoes. Each echo signal was individually phase encoded, by applying phase encoding gradients after each 180° RF pulse and using rewinders to minimize artifacts (23). A 128 ms echo was symmetrically acquired using a spectral width of 2000 Hz. A 32 × 32 circular k-space sampling scheme was applied, using a 24 × 24 cm field-of-view (FOV). Figure 1d shows schematically how k-space was scanned by phase encoding each of the spin-echoes. The particular scanning scheme resulted in an effective echo time of 200 ms. During each

MRM 30:409–414 (1993)

From the Laboratory of Diagnostic Radiology Research, National Institutes of Health, Bethesda, Maryland (J.H.D.), and in Vivo NMR Research Center, BEIP, NCRR, National Institutes of Health, Bethesda, Maryland (J.H.D., C.T.W.M.).

Address correspondence to: Jeff H. Duyn, Laboratory of Diagnostic Radiology Research, National Institutes of Health, Building 10, Room B1N-256, Bethesda, MD 20892.

Received March 5, 1993; revised June 11, 1993; accepted June 21, 1993.

1993 SMRM Young Investigator's Award Finalist.

0740-3194/93 $3.00

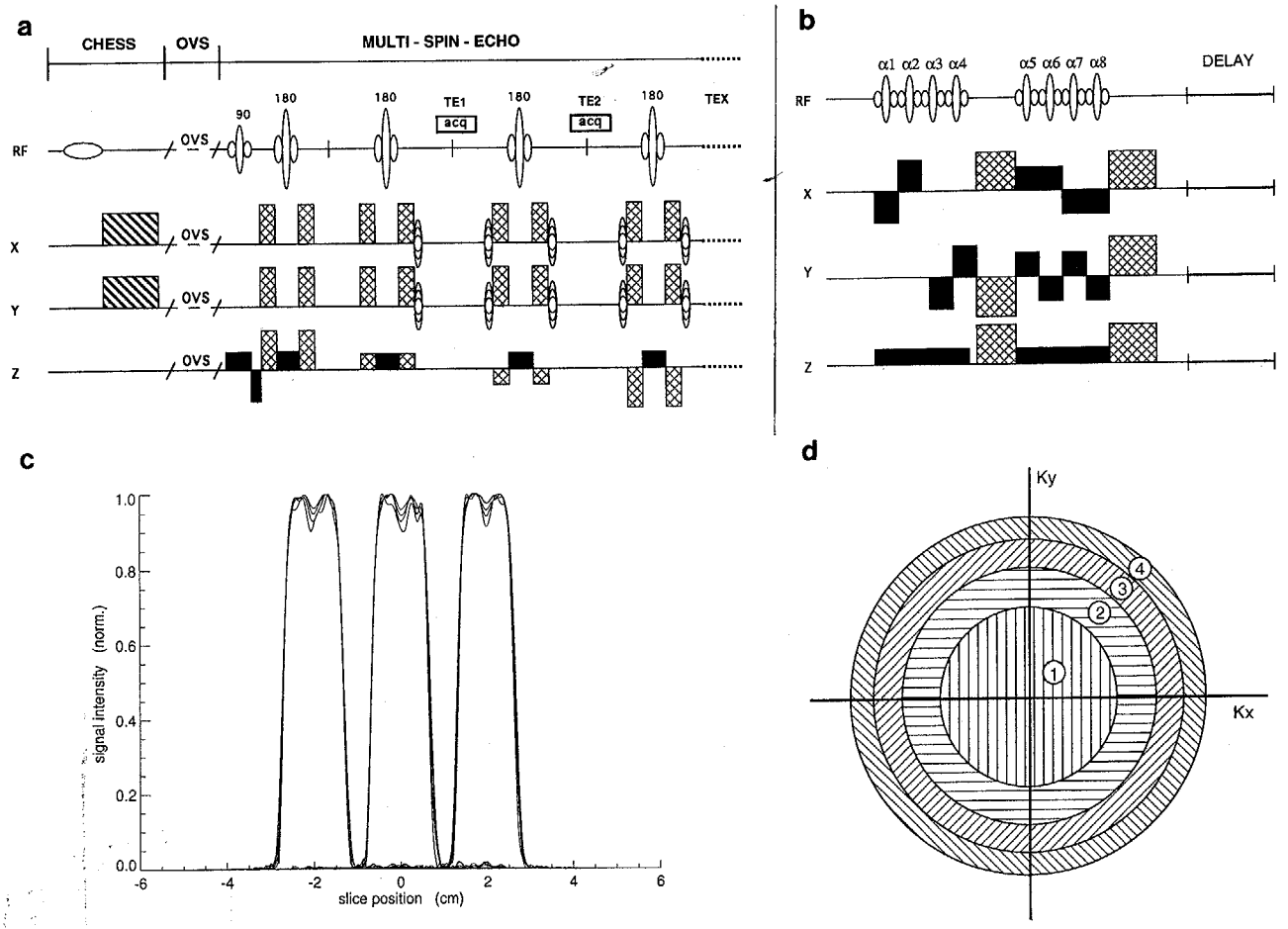

FIG. 1. (a) Schematic diagram of multi-echo HSI pulse sequence. The sequence combines CHESS water suppression and multiple-slice outer volume suppression (OVS, see Fig. 1b) with a multi-spin-echo data acquisition sequence. Spin-echoes are generated and acquired in intervals (*acq*) between 180° RF pulses at echo times *TE*1, *TE*2, . . .*TEX*. All of the RF pulses are slice-selective and select the same axial slice. The 180° pulses are flanked by gradient crushers to suppress unwanted signal. Gradient phase encoding is performed in each acquisition interval and phase encoding rewinders are used to minimize artifacts due to unwanted coherences. The complete sequence acquires four spin-echoes and is repeated for each of the three slices studied. (b) Schematic diagram of the OVS pulse sequence. The sequence suppresses water and lipid signals from octagonally grouped slices around the VOI, using eight slice-selective RF pulses (α1-α8). The pulses are combined in two groups of four. The first group suppresses slices left, right, anterior, and posterior with respect to the VOI and is followed by a 6-ms gradient crusher. The second group of four pulses suppresses the diagonal oriented slices and is followed by an 8-ms gradient crusher. The crushers have the specific orientation indicated in the diagram in order to minimize creation of coherences. The amplitudes of the RF pulses are fine-tuned to compensate for T_1 relaxation. A delay is appended to minimize the effects of short-term eddy currents on the spin-echo sequence. (c) The positions and profiles of the slices studied in the multi-spin-echo experiment, determined by phantom measurements. Plotted for each echo and each slice is the signal intensity as a function of the distance in axial direction (perpendicular to the slice). All signals are scaled to unity in order to correct for signal losses due to pulse angle imperfections and T_2 relaxation. The similarity between profiles of subsequent echoes is shown in largely coincident plots. (d) Segmentation of *k*-space used in the multi-spin-echo sequence. Each of the four segments is covered by the encoding of a particular echo. The segments are numbered according to the successive acquisition intervals.

experiment, data during one *TR* period was acquired without phase encoding gradients in order to provide correction factors for signal losses due to T_2 relaxation and to RF pulse angle and slice profile imperfections (data processing). Three slices were acquired within a total *TR* of 2700 ms. The total HSI measurement time was 9 min.

Protocol

Before the HSI experiment, axial gradient-echo (GRASS) images were obtained with $TE = 30$ ms, $TR = 600$ ms, to locate the skull/brain interface. On the basis of these images, the VOI was selected and the OVS pulses were positioned. Localized shimming was then performed over the VOI and the RF amplifier output was adjusted using a single spin-echo sequence. The RF pulse amplitude of the CHESS water suppression pulse was adjusted using the multi-echo sequence, by minimizing water signals in the first echo ($TE = 200$ ms). Then the multi-echo HSI experiment was started, and upon completion, a series of axial GRASS MR images was obtained with $TE = 30$ ms, $TR = 600$ ms, using a slice thickness and location corresponding with the HSI images. The total measurement time, including GRASS MRI scans, was 20 min. For

comparison, a standard single-echo multi-slice acquisition (6) was performed on the same volunteer, with TE = 272 ms and slightly modified amplitudes of CHESS and OVS RF pulses. A TR of 2200 ms was chosen, resulting in an amount of T_1 weighting similar as in the multi-echo experiment. The total measurement time for the single-echo HSI experiment was 27 min.

Data Processing

Data processing was performed off-line on a SUN-SPARC workstation using IDL™ software (Research Systems Inc., Boulder, CO). Each slice was processed separately.

For the multi-echo experiment, the four echoes of the reference acquisition (acquired without phase encoding gradients) were apodized with a 10% Hamming filter and Fourier transformed, resulting in total volume spectra from each of the four echoes. The magnitude signals of the NAA resonance were used to calculate correction factors for signal losses due to T_2 relaxation and imperfections in RF pulse angle and slice profiles. Signal losses during each 180° RF pulse were in the order of a few percent, and the correction for the combined effects of relaxation and RF pulse angle corresponded to an exponential decay constant of 400 ms. The correction factors were applied to data of the phase encoded experiment, after which a 10% Hamming filter was applied in spectral domain, and a radial cosine filter in the spatial domain (2D filter). The data matrix was then zero-filled eight times in the spectral domain, and Fourier transformed in all three dimensions. The resulting effective in-plane spatial resolution was 1.3 cm, as calculated from the 2D point spread function (PSF) (see Figs. 3a and 3c) at half maximum height, and included effects of the circular k-space sampling scheme. Spectra were corrected for B_0 inhomogeneities by referencing to the position of NAA. In case of NAA being below an optional threshold, its position was taken from neighbouring voxels. Metabolite images of NAA, and choline + creatine were created by integrating the spectra between 1.9 ppm and 2.1 ppm and between 2.9 ppm and 3.3 ppm, respectively.

For the standard single-echo multi-slice experiment, a cosine filter was applied in spectral domain, whereas the spatial domain was filtered identically as the multi-echo data set. Also peak-picking and integration were performed in an identical fashion as with the multi-echo data set.

RESULTS

The results of the multi-echo multi-slice experiment are summarized in Figs. 2a–2d, and spectroscopic images obtained with the conventional single-echo multi-slice experiment are shown in Fig. 2b.

Figure 2a shows, for each of the three slices studied, the spectroscopic images of NAA and total choline + total creatine, together with the corresponding GRASS images. Clearly recognizable in the two most inferior slices (top rows) are the ventricular spaces. The bright intensities in the NAA images are insufficiently suppressed signals of lipid from the skull area, which occasionally bleed into brain regions (e.g., slice 1). The bright intensities in the choline + creatine images from top and bottom slices are caused by residual water signal.

Results of the single-echo multi-slice experiment are presented in Fig. 2b. As can be seen from the GRASS images, the subject was somewhat displaced in craniocaudal direction, resulting in a slice selected at a more superior location. The metabolite images show a delineation of anatomical details comparable to the multi-echo images. There is clearly less lipid in the NAA images.

The SNR of the images of the multi-echo experiment and the single echo experiment is comparable, and varies between 15 and 20 for the NAA images and between 10 and 15 for choline + creatine images. The spectral quality of the multi-echo experiment is demonstrated in Fig. 2c, which shows an array of spectra extracted from a region just left of the ventricles in slice 2. For comparison, an individual spectrum is taken from this array (second from left in top row) and displayed in Fig. 2d, together with the corresponding spectrum of the single-echo experiment (extracted from the same position in image matrix).

DISCUSSION

The results presented above demonstrate the feasibility of fast spectroscopic imaging using the multi-spin-echo method. The resolution and SNR of the spectroscopic images are comparable to those of conventional single echo HSI images. Due to the reduced echo sampling times, the spectral resolution is somewhat degraded. Also the spectral SNR suffered some loss, especially in areas with excellent B_0 homogeneity. This loss was not reflected in the images because for both single- and multi-echo experiments the same spectral integration widths were used. Reducing this width for the single-echo experiment would increase its sensitivity to susceptibility effects, and cause signal loss in areas with poor B_0 homogeneity. The multi-echo experiment is less sensitive to susceptibility effects in the sense that there is less variation in line width. In the following other aspects of the multi-echo technique are discussed:

Number of Echoes

An important design choice in the multi-echo experiment is the number of echoes. A larger number of echoes gives a potentially higher efficiency. Because the total acquisition time (echo duration × number of echoes) is limited by T_2, an increased number of echoes is accompanied by a reduced echo duration. Reducing the echo duration below T_2^* (over the voxel), will lead to a reduction in spectral resolution, and only a minimal increase in efficiency. Therefore, the optimum number of echoes, with respect to efficiency and spectral resolution, depends on the ratio T_2^*/T_2, and therefore on the B_0 homogeneity. In the experiment described above we have acquisition time = 128 ms T_2^* and $T_2^*/T_2 < 0.5$ for choline, creatine and NAA. With four echoes, we are measuring at close to the optimum efficiency. In regions of particularly poor B_0 homogeneity the optimum efficiency will be reached at a higher number of echoes.

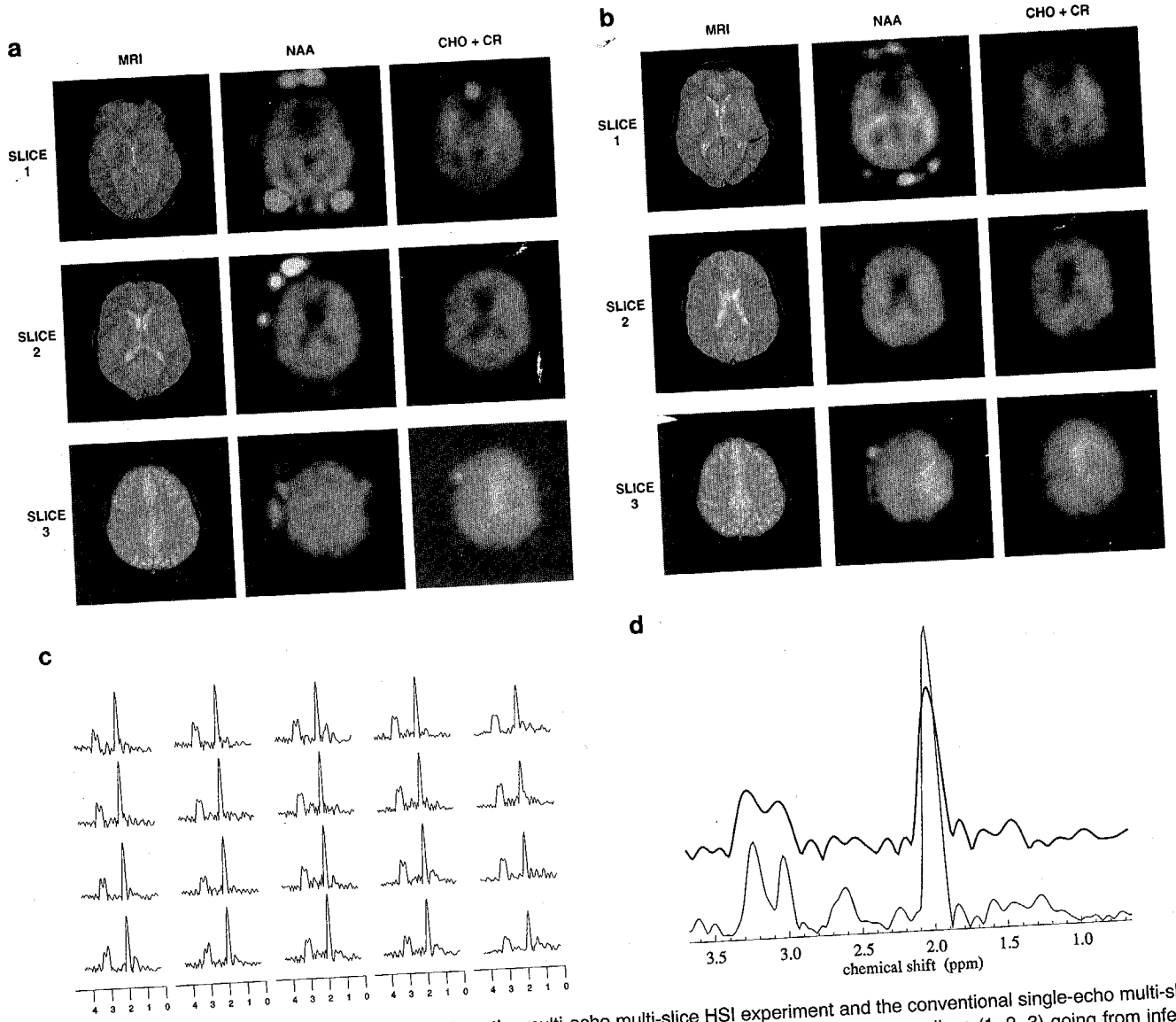

FIG. 2. GRASS MRIs and metabolite images from the multi-echo multi-slice HSI experiment and the conventional single-echo multi-slice experiment. Each of the figures (a and b) displays three rows of images corresponding to subsequent slices (1, 2, 3) going from inferior to superior through the brain. Each row shows GRASS MRI and NAA and choline + creatine metabolite images. (a) Multi-echo experiment; (b) single-echo experiment. (c) Array of spectra, obtained with the multi-echo HSI experiment. The spectra were extracted from slice 2, from a region left of the ventricles. Clearly distinguishable is the resonance of NAA and the overlapping resonances of choline and creatine. The suppression of lipid and water signals in these spectra appears reasonable. (d) Comparison of spectral quality achieved with multi-echo (top spectrum) and single-echo (bottom spectrum) experiments. A spectrum from the array of Fig. 2c (second spectrum from top row) is compared with a spectrum, extracted from the same position in slice 2 of the single-echo experiment.

Phase Distortions

During initial tests of the multi-echo experiment on phantoms artifacts were seen associated with transitions in the signal phase going from one segment in k-space to the next. Most of these artifacts could be explained by eddy current induced residual gradients and B_0 shifts, originating from CHESS and OVS gradient crushers, and resulting in an accumulated signal phase at the center of the first acquisition period. This additional phase is inverted in subsequent echoes, leading to the artifacts. For example a net accumulation of 30° phase in the interval between the 90° RF pulse and the first acquisition interval, due to a B_0 shift, leads to significant distortion of the PSF. This is demonstrated in Figs. 3a and 3b which show the PSF for the multi-echo experiment without (Fig. 3a) and with (Fig. 3b) a position independent phase distortion of 30°. In order to minimize phase distortions in the echo signals, a delay of 6 ms was used between OVS and spin-echo sequence. Furthermore, the amplitudes of the crusher gradients after the 180° RF pulses were fine-tuned to minimize net dephasing at the centers of the acquisition intervals. This was done once for a specific setting of timing variables (*TR*, delays after CHESS and OVS, *TE*s) and gradient strengths (crushers, slice selection gradients). Remaining phase differences between echoes were negligible and caused no visible artifacts.

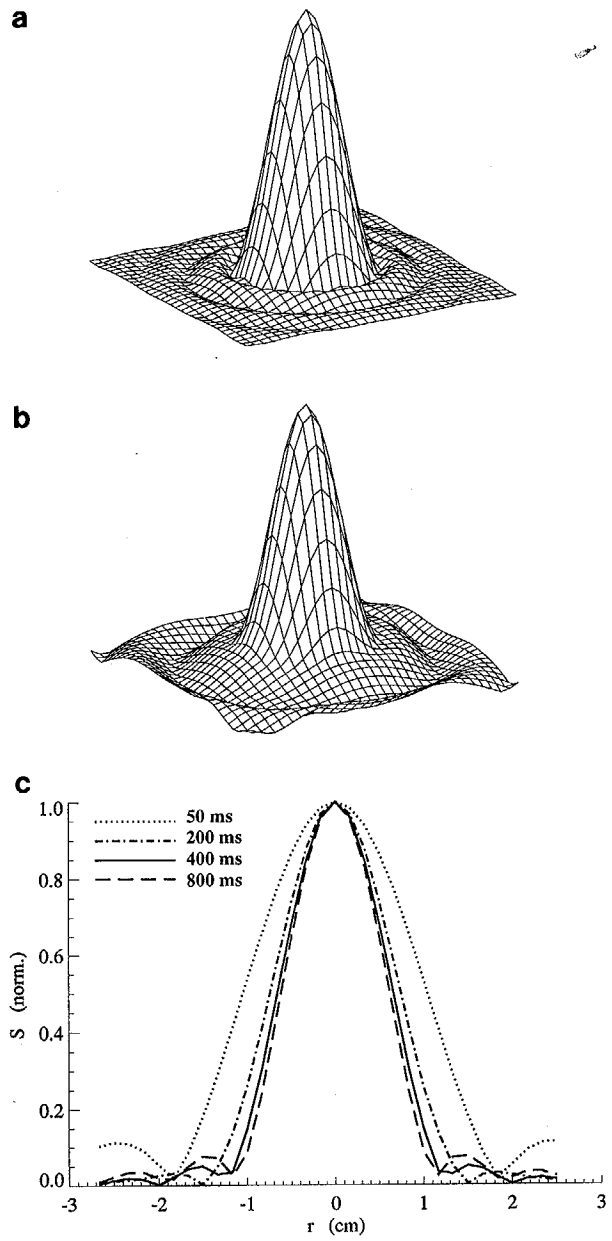

FIG. 3. Simulated 2D PSF (absolute value) of the multi-echo HSI experiment, after spatial apodization and corrected for effects of circular *k*-space sampling. (b) Simulated 2D PSF (absolute value) of the multi-echo HSI experiment (cf. Fig 2a), assuming 60° phase alternation (+30,–30, ..) between subsequent echoes. (c) Simulated one-dimensional profiles of the PSF for different correction factors used for exponential decay over subsequent echoes. Plotted are absolute signal values as a function of the radial distance *r*. The decay time constant was 400 ms. Simultated are PSFs after application of corrections equivalent to decay time constants of 50, 200, 400, and 800 ms.

T_2 Effects on Resolution

During data processing, each echo was multiplied by a correction factor, to compensate for signal losses due to T_2 relaxation and RF pulse imperfections. The correction factor used in our experiments was determined by measuring the NAA signal decay over the four echoes, and corresponded to a T_2 of 400 ms. Reports have shown that in normal brain T_2 relaxation times of choline, creatine, and NAA vary between 200 and 400 ms (24, 25). Because *k*-space is scanned in a segmented fashion (Fig. 1d), inappropriate correction for T_2 relaxation effects would result in distortion of the spatial PSF. This is demonstrated in Fig. 3c, which shows simulated 1D profiles of the PSF for different actual T_2 values, but using a single correction factor corresponding to a T_2 of 400 ms. The PSF for T_2's between 200 and 800 ms is very similar, and suggests the adequacy of a single correction factor for choline, creatine, and NAA. In using this correction, components of lipid resonances with short T_2 ($T_2 < 50$ ms, (26)) have a much broadened PSF with increased sidelobe amplitudes (Fig. 3c).

Contamination by Lipid Signals

The multi-echo method showed an increased sensitivity to contamination by lipid signals as compared with its single echo counter part. Possible explanations are the following. First, the component of lipid with the short T_2 has a broadened spatial PSF, as discussed in the previous section. Also, the short T_2 component of lipid is still quite intense at *TE*'s around 200 ms, and has a larger contribution to the spectrum than at $TE = 272$ ms. And finally, the spectral PSF is broadened due to the reduced echo duration. This increases the risk of contamination of the NAA image by lipid signals because their resonances are close together in the spectrum. Therefore, special attention must be paid to the choice of the VOI, and the positioning and adjustment of the OVS pulses.

Measurement of Lactate

The application of multi spin-echo spectroscopy described in this work was not aimed at measuring lactate. The lactate signal originates from a coupled methyl doublet, with a phase varying with echo time. In order to measure the doublet in phase, echo times have to be multiples of 136 ms. For lactate to be measured without localization errors, subsequent echo times have to be separated by a multiple of 272 ms. An experiment with echo times of 136, 408, 680, and 952 ms could be feasible because lactate has a T_2 of around 1200 ms (24). However, in the later echoes, the other metabolites of interest will be attenuated significantly due to their much shorter T_2 values, and will therefore have broadened PSFs.

In the experiment discussed above, the increased efficiency of the multi-echo technique was used to reduce the measurement time. Alternatively, the increased efficiency could be used to create T_2 maps (by scanning all of *k*-space with each echo), or to perform a full 3D experiment. For example an experiment with $20 \times 20 \times 12$ encoding steps (cylindrical *k*-space sampling) at $TR = 2$ s would take 30 min. Using a $20 \times 20 \times 12$ cm FOV an isotropic (nominal) resolution of $1 \times 1 \times 1$ cm is achieved. Both experiments are currently being developed.

CONCLUSION

The multi-slice multi-echo HSI technique discussed in this paper demonstrated a threefold reduction in

measurement time as compared with single echo HSI. Multiple slice HSI studies were performed within 20 min, including setup times. We presented metabolite images of NAA and choline + creatine with 1.7 cc spatial resolution and a SNR comparable with conventional HSI techniques. The SNR and resolution of the spectra obtained with the multi-echo experiment was somewhat degraded, which was especially apparent in the overlap of the choline and creatine resonances. Spectral peak-fitting or time domain spectral fitting may alleviate this problem.

ACKNOWLEDGMENTS

The authors thank Joe Gillen, Daryl Despres, Geoffrey Sobering, and Peter van Zijl for assistance and discussions.

REFERENCES

1. D. Spielman, J. Pauly, A. Macovski, D. Enzmann, *Magn. Reson. Med.* **19,** 67 (1991).
2. C. T. W. Moonen, G. Sobering, P. C. M. van Zijl, J. Gillen, M. von Kienlin, A. Bizzi, *J. Magn. Reson.* **98,** 556 (1992).
3. S. Posse, B. Schuknecht, M. E. Smith, P. C. M. van Zijl, N. Herschkowitz, C. T. W. Moonen, *J. Comput. Assist. Tomogr.* **17–1,** 1 (1993).
4. J. H. Duyn, G. B. Matson, A. A. Maudsley, M. W. Weiner, *Magn. Reson. Imag.* **10,** 315 (1992).
5. C. T. W. Moonen, G. Sobering, P. C. M. van Zijl, J. Gillen, P. Daly, *in* "Proceedings, 9th Annual Meeting, Society of Magnetic Resonance in Medicine, 1990," p. 139.
6. J. H. Duyn, J. Gillen, G. Sobering, P. C. M. van Zijl, C. T. W. Moonen, *Radiology*, in press.
7. D. Spielman, J. M. Pauly, A. Macovski, G. Glover, D. R. Enzmann, *J. Magn. Reson. Imaging* **2,** 253 (1992).
8. P. R. Luyten, P. C. van Ryen, C. A. F. Tulleken, J. A. den Hollander, *in* "Proceedings, 8th Annual Meeting, Society of Magnetic Resonance in Medicine, 1989," p. 452.
9. J. H. Duyn, G. B. Matson, A. A. Maudsley, J. W. Hugg, M. W. Weiner, *Radiology* **183,** 711 (1992).
10. D. L. Arnold, P. M. Matthews, G. Francis, J. Ante, *in* "Proceedings, 10th Annual Meeting, Society of Magnetic Resonance in Medicine, 1991," p. 80.
11. C. A. Husted, J. W. Hugg, J. H. Duyn, G. B. Matson, A. A. Maudsley, M. W. Weiner, *in* "Proceedings, 10th Annual Meeting, Society of Magnetic Resonance in Medicine, 1991," p. 83.
12. P. R. Luyten, P. C. van Ryen, L. C. Meinert, A. J. H. Marien, J. A den Hollander, *in* "Proceedings, 9th Annual Meeting, Society of Magnetic Resonance in Medicine, 1990," p. 1009.
13. P. R. Luyten, A. J. H. Marien, W. Heindel, P. H. J. van Gerwen, K. Herholz, J. A. den Hollander, G. Friedmann, W. D. Heiss, *Radiology* **176,** 791 (1990).
14. K. Herholz, W. Heindel, P. R. Luyten, J. A. Den Hollander, U. Pietrzyk, J. Voges, H. Kugel, G. Friedman, W.-D. Heiss, *Ann. Neurol.* **31,** 319 (1992).
15. M. J. Fulham, A. Bizzi, M. J. Dietz, H.-L. Shih, R. Raman, G. S. Sobering, J. A. Frank, A. J. Dwyer, J. R. Alger, G. Di Chiro, *Radiology* 185, 675 (1992).
16. D. J. Meyerhoff, J. H. Duyn, L. Bachman, G. Fein G, M. W. Weiner, *in* "Proceedings, 10th Annual Meeting, Society of Magnetic Resonance in Medicine, 1991," p. 404.
17. A. A. Maudsley. *J. Magn. Reson.* **68,** 363 (1986).
18. J. Hennig, A. Nauerth, H. Friedburg, *Magn. Reson. Med.* **3,** 823 (1986).
19. L. E. Crooks, M. Arakawa, J. Hoenninger, J. Watts, R. McRee, L. Kaufman, P. L. Davis, A. R. Margulis, J. de Groot, *Radiology* **143,** 169 (1982).
20. C. M. J. van Uijen, J. H. den Boef, F. J. J. Verschuren, *Magn. Reson. Med.* **2,** 203 (1985).
21. E. M. Haacke, F. H. Bearden, J. R. Clayton, N. R. Lingar, *Radiology* **158,** 521 (1986).
22. J. H. Duyn, J. H. N. Creyghton, J. Smidt, *in* "Proceedings, 3rd Annual Meeting, Society of Magnetic Resonance in Medicine, 1984," p. 177
23. J. Frahm, K. D. Merboldt, W. Haenicke, *J. Magn. Reson.* **27,** 307 (1987).
24. J. Frahm, H. Bruhn, M. L. Gyngell, K. D. Merboldt, W. Haenicke, R. Sauter, *Magn. Reson. Med.* **11,** 47 (1989).
25. P. Gideon, O. Henriksen, *Magn. Reson. Imag.* **10–6,** 983 (1992).
26. R. L. Kamman,. C. J. G. Bakker, P. van Dijk, G. P. Stomp, A. P. Heiner, H. J. C. Berendsen, *Magn. Reson. Imaging* **5,** 381 (1987).